NASA CR-66246

REVIEW OF A DSIF DATA TAKING AND ORBIT DETERMINATION METHOD

By R. D. Elliott

Prepared under Contract No. NAS 1-4605-7 by
TRW Systems

for

NATIONAL AERONAUTICS AND SPACE ADMINISTRATION

REVIEW OF A DSIF DATA TAKING AND ORBIT DETERMINATION METHOD

By R. D. Elliott

Prepared under Contract No. NAS 1-4605-7 by
TRW Systems

for

NATIONAL AERONAUTICS AND SPACE ADMINISTRATION

SUMMARY

This report presents a review of some of the characteristics of the Deep Space Instrumentation Facility (DSIF) as it applies to the determination of lunar orbits and the solution of lunar gravitational potential constants. The capability of the DSIF to determine orbital parameters and lunar potential constants can be analyzed in terms of the errors commited in the links of the data chain from sensor to the determined orbital parameters. The task which led to this report was a careful reading through Jet Propulsion Laboratory (JPL) and related documentation to clearly understand the basis of JPL's estimates of standard errors in DSIF counted doppler and range measurements.

The results obtained in this report parallel those reflected in the accuracy estimates made by JPL in their reports and description of the DSIF, and it is concluded that the DSIF should indeed have the capability required to perform lunar orbiting mission data gathering and analysis. The data used in this report were taken from JPL reports on the Ranger VI and Ranger VII missions.

CONTENTS

		Page
1.	INTRODUCTION	1
2.	LUNAR ORBITER	3
3.	WEIGHTED LEAST SQUARES	4
4.	JPL WEIGHTS	4
5.	ERROR SOURCES FOR TWO-WAY DOPPLER	5
6.	RELATIVISTIC EFFECTS ON TWO-WAY DOPPLER	16
7.	UNCERTAINTY CONTRIBUTED BY ASSIGNING A RANGE RATE INTERPRETATION TO THE COUNTED DOPPLER MEASUREMENT AND THE ASSIGNMENT OF TIME	18
8.	CALCULATION OF QUANTIZATION OF COUNT AND COUNT RATE DATA	20
9.	EFFECT OF BIAS ON DETERMINATION OF LUNAR GRAVITY	20
10.	RANGE MEASUREMENTS	22
11.	POWER SPECTRAL ANALYSIS	22
12.	SPACE PLASMA EFFECTS	29
13.	CONCLUSIONS	29
14.	BIBLIOGRAPHY	29

ILLUSTRATIONS

		Page
1.	Schematic Diagram of an ODP Filter	2
2.	Station 51 Pass No. 01/301 Premaneuver Residuals (16:21 GMT)	7
3.	Station 51 Pass No. 01/303 Premaneuver Residuals	9
4.	Residuals for Doppler Data Without ODP Refraction Model (Elevation Rate 0.245 deg/min)	13
5.	Station 12 Post Maneuver Pass No. 2 Two-Way Doppler Residuals (Start 07:18 GMT).	14
6.	Station 12 Post Maneuver Pass No. 2 Two-Way Doppler Residuals (Start 13:18 GMT).	15
7.	Power Spectra and Autocorrelation — Case 16	23
8.	Power Spectra and Autocorrelation — Case 18	24
9.	Power Spectra and Autocorrelation — Case 17	25
10.	Power Spectra and Autocorrelation — Case 23	26

TABLES

		Page
I.	Sensitivity Coefficients, g_i, for HA, DEC and Two-Way Doppler	6
II.	Runs of Four and Six Iterations on Known "A Priori" Trajectory	21
III.	Statistics on Post Maneuver Data	27
IV.	Values of Estimated Parameters at Maneuver Epoch . . .	28

1. INTRODUCTION

A brief discussion of the errors associated with tracking data taken by the Deep Space Instrumentation Facility (DSIF), engineered and operated by Jet Propulsion Laboratories, is contained in this note. The rough theoretical calculations of error sources are intended more to serve to increase the confidence level of empirically derived behavior and values.

For the high frequency "noise" region, the doppler residual plots from ODP runs on such data as that from Pioneer VI and Pioneer VII exhibit some information on the magnitude of the errors committed by the total system. Spectral and covariance analysis of some of the residual time series are presented. It would be a mistake to assume that residuals reflect the total picture, since the ODP, viewed as a filter,* accepts "noise" (errors) lying within its band-pass and rejects "noise" as well as valid information which lies outside its band-pass. Thus some "noise" is lost or passed into the orbit by the ODP. An example of such "noise" would be that of an absolute timing error which is lost into the computed orbit with no way of computing its magnitude within the ODP. The "transfer function" of the ODP depends upon the models contained within it and the mode in which it is used. For example, if data from several stations are processed together, it becomes theoretically possible to solve for or "filter out" time or oscillator biases, drifts, etc., of all stations relative to some master station which must be assumed to be synchronized to ephemeris time (to the known accuracy of the ephemeris). In the latter case, the transfer function would no longer extend to zero frequency, but would have a low frequency rolloff as well as a high frequency cutoff.

*For conceptual purposes here we neglect problems of the inherent non-stationarity of the process and view of ODP as a data filter with a definite transfer function. A more rigorous treatment is possible in terms of the covarience matrices used in the ODP. Implementation of such an approach, however, would require many computer runs as analytic solutions are no longer possible. This would be outside the scope of this study.

There are, then, two basic classes of errors. The first contains those errors which occur because the ODP's bandpass rejects part of the information spectrum. (This results when the models in the ODP are inadequate to simulate reality, and the covariance and spectrum analysis on the residuals are intended to detect errors of this class.) The second class contains those errors which occur because the noise spectrum shares a common region with the ODP transfer function, and thus the noise is accepted as information and included in the orbit. To some extent at least, this, too, is an inadequacy in modeling or an inadequacy in the amount of data processed. See Figure 1 for a more schematic presentation of the above ideas. The "bandpass characteristics" of the filter depend on model accuracy and amount (in time) and amount (in type) of data. This will vary from mission to mission in the latter categories as well as the model accuracy category, since time dependent changes in the physical environment do occur.

Thus the required information is partially contained in the residuals, and partially derived from estimates (experimental and theoretical) of the modeling accuracy.

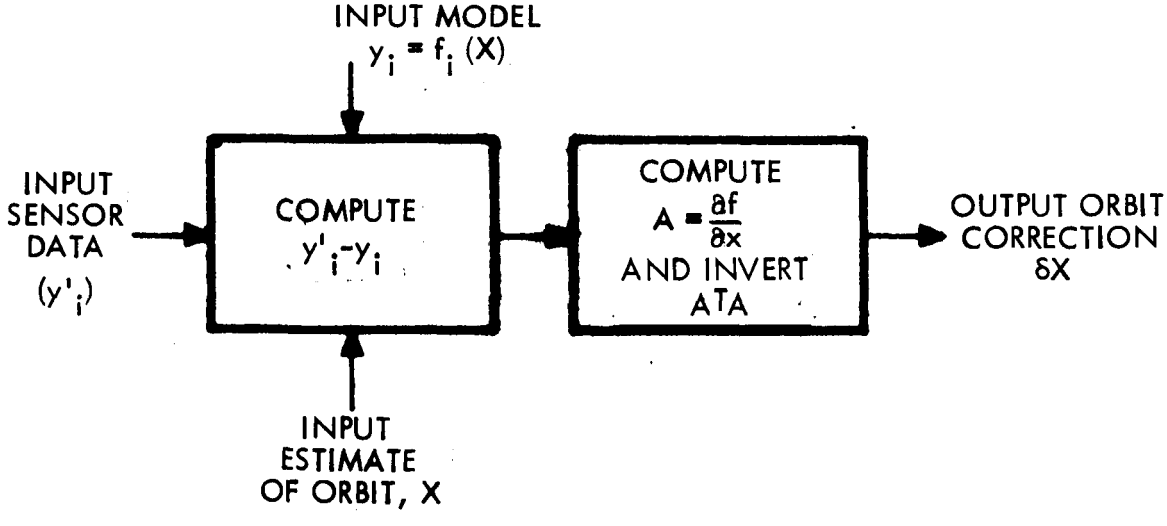

Figure 1. Schematic Diagram of an ODP Filter

The data are fit in a least squares sense to a model of the physical phenomenological processes represented by f_i and the orbit, x, is corrected by δx; and the process is continued (iterated) until δx changes by a sufficiently small amount.

ODP FILTER ANALOG

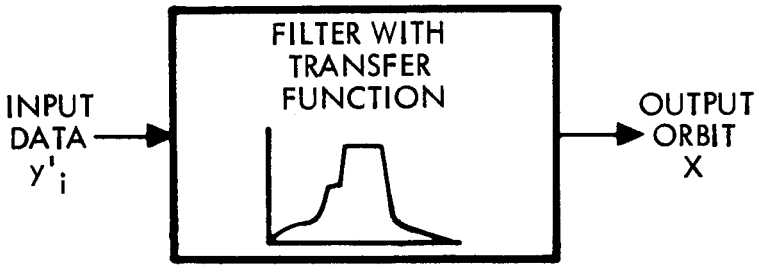

However, y_i' contains, in addition, physically additive noise n, such that $y_i' = x + n$. If the ODP was perfect it would reject n and pass x, but in practice only part of n is rejected. Furthermore the filter does not quite match reality, and so it contributes a noise n'. Thus instead of obtaining x we obtain $x + n' + p(n)$ where p(n) is some portion of n. Therefore the residuals δy, while ideally equal to n the noise or inaccuracy in the measurements, are modified to give $\delta y = n' + q(n)$, where q(n) is that portion of n which is rejected by the filter. Hence we are examining the residuals for q(n) and n', while trying to estimate p(n). Proper interpretation of these quantities permits an estimate of system accuracy.

2. LUNAR ORBITER

For the purposes of Lunar Orbiter, the problem becomes narrowed to a consideration of two-way doppler, and angle data. All JPL DSIF stations are assumed to be equipped with rubidium time standards which drive the VCO's. The a priori data weighting scheme employed by JPL is briefly summarized below, and the following discussion will be with reference to this weighting scheme.

3. WEIGHTED LEAST SQUARES

In the weighted least-squares differential correction ODP, it is necessary to have an a priori covariance matrix of the data. The assumption usually made then is that the weighting matrix is the inverse of the covariance matrix. The covariance matrix of the estimated orbit parameters under these assumptions is given by:

$$\left(A^T W A\right)^{-1} = \left(A^t \Sigma^{-1} A\right)^{-1}$$

Where A is the normal matrix containing the partial derivatives of the entire ODP model, A^T is the transpose of A, W is the weighting matrix, and Σ is the covariance matrix of the observations and is equal to the inverse of W by definition.

4. JPL WEIGHTS

The a priori weights used by JPL in these ODP are according to the following scheme.

The effect variance of a particular data-type is given by:

$$\sigma^2 = \sum_{i=1}^{6} S_i^2 g_i^2 \, \mathrm{MAX}\left(1, \frac{T_c}{T_s}\right)$$

where

i = basic error source

S_i^2 = variance of basic error source

g_i^2 = sensitivity coefficient of a particular data-type on the ith basic error source

MAX (a, b) = the larger of the two numbers a, b

T_c = correlation width (in seconds) of the basic error source

T_s = sample spacing in seconds

The error sources and identifying index values i are:

Error Source	Index Value i
Computing error	1
Rounding error	2
Oscillator drift rate	3
Added or dropped cycles	4
Refraction correction	5
Spacecraft tumbling	6

5. ERROR SOURCES FOR TWO-WAY DOPPLER

a) Errors in the orbit determination due to trajectory computation round-off errors in the Cowell integrations method.

Errors of this type tend to accumulate with time along the trajectory and thus give rise to a drift-type dependent "noise." Unfortunately, this type of noise is apparently lost from the residuals, which is reasonable since the ODP would tend to pass this type of error into the orbit.

b) Rounding error caused by the start and stop count pulses not necessarily occurring at times such that an integral number of cycles has passed.

This error tends to show up as "high frequency noise" and is relfected in the residuals, giving higher standard deviations.

Figure 2 illustrates round-off error on doppler data taken over 5-second intervals as compared to 60-second intervals, for which latter case the round-off error is below other sources ($<10^{-2}$ cps). Although the 5-second doppler data are of extremely short sample length, a peak deviation equal to the theoretical occurred once within this sample.

TABLE I. —SENSITIVITY COEFFICIENTS, g_i, FOR HA, DEC AND TWO-WAY DOPPLER*

Error source	Sensitivity coefficient		
	Hour angle	Declination	Two-way doppler
1	1/cos (Dec)	1	1
2	1	1	$1/T_c$
3	1	1	ρ/c
4	Δr (HA)	Δr (Dec)	$1/\sqrt{3T_c}$
5	— —	— —	$\Delta r \dot{\rho}$
6	— —	— —	1

$$\Delta r\,(\mathrm{HA}) = \frac{\cos\phi \sin^2(\mathrm{HA})}{\cos^2\gamma \sin\sigma}\,(\Delta r\,\gamma)$$

$$\Delta r\,(\mathrm{Dec}) = \frac{\cos\gamma \sin\phi - \sin\gamma \cos\phi \cos\sigma}{\cos(\mathrm{Dec})}\,(\Delta r\,\gamma)$$

ϕ = geocentric latitude of tracking station

γ = elevation angle

σ = azimuth angle

$\Delta r\gamma$ = refraction correction for elevation angle

= $57.2957795\ n\ b_1 b_2/340.0$, for $\gamma < 0.3$ rad

= $57.2957795\ n \times 10^{-6} \cot\gamma$, for $\gamma \geq 0.3$ rad

n = index of refraction, nominally 340.0

$b_1 = 1.0 - (1.216 \times 10^5\, b_3\, \gamma) - (51.0 - 300.0\,\gamma)\sqrt{b_3}$

$b_2 = [7.0 \times 10^{-4}/(0.0589 + \gamma)] - 1.26 \times 10^{-3}$

$b_3 = 1/10^3\,(r - RE)$

r = geocentric radius to spacecraft

RE = Earth's radius

$\Delta r\dot{\rho} = 0.0018958\ [(\sin A + 0.06483)^{-1.4} - (\sin B + 0.06483)^{-1.4}]\ n/340.0$

$A = \gamma + T_c\,\dot{\gamma}/2$

$B = \gamma - T_c\,\dot{\gamma}/2$

T_c = doppler count interval, sec

ρ = range from station to spacecraft

*From Reference 1, page 9

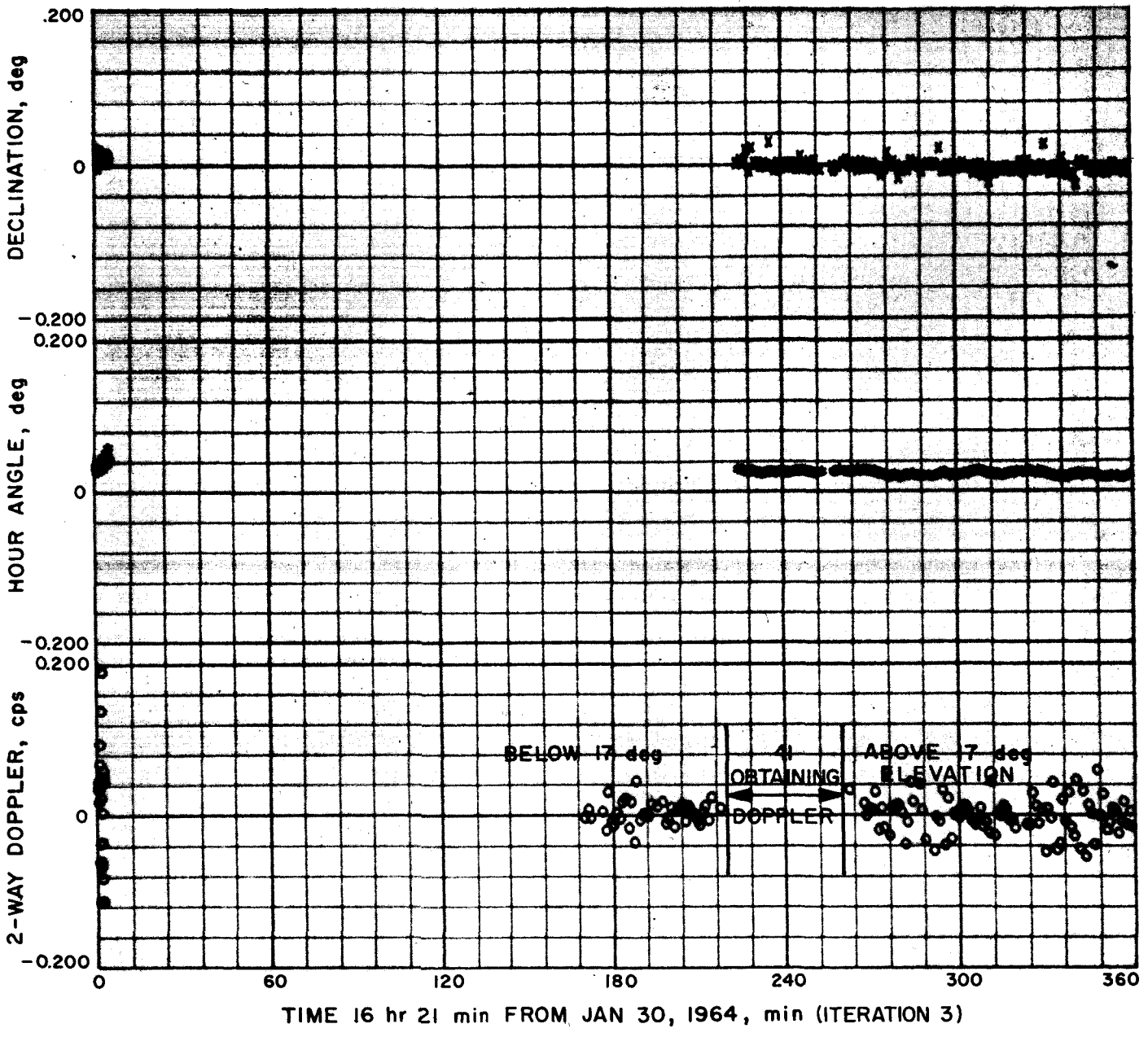

Figure 2. Station 51 Pass No. 01/301 Premaneuver Residuals (16:21 GMT)*

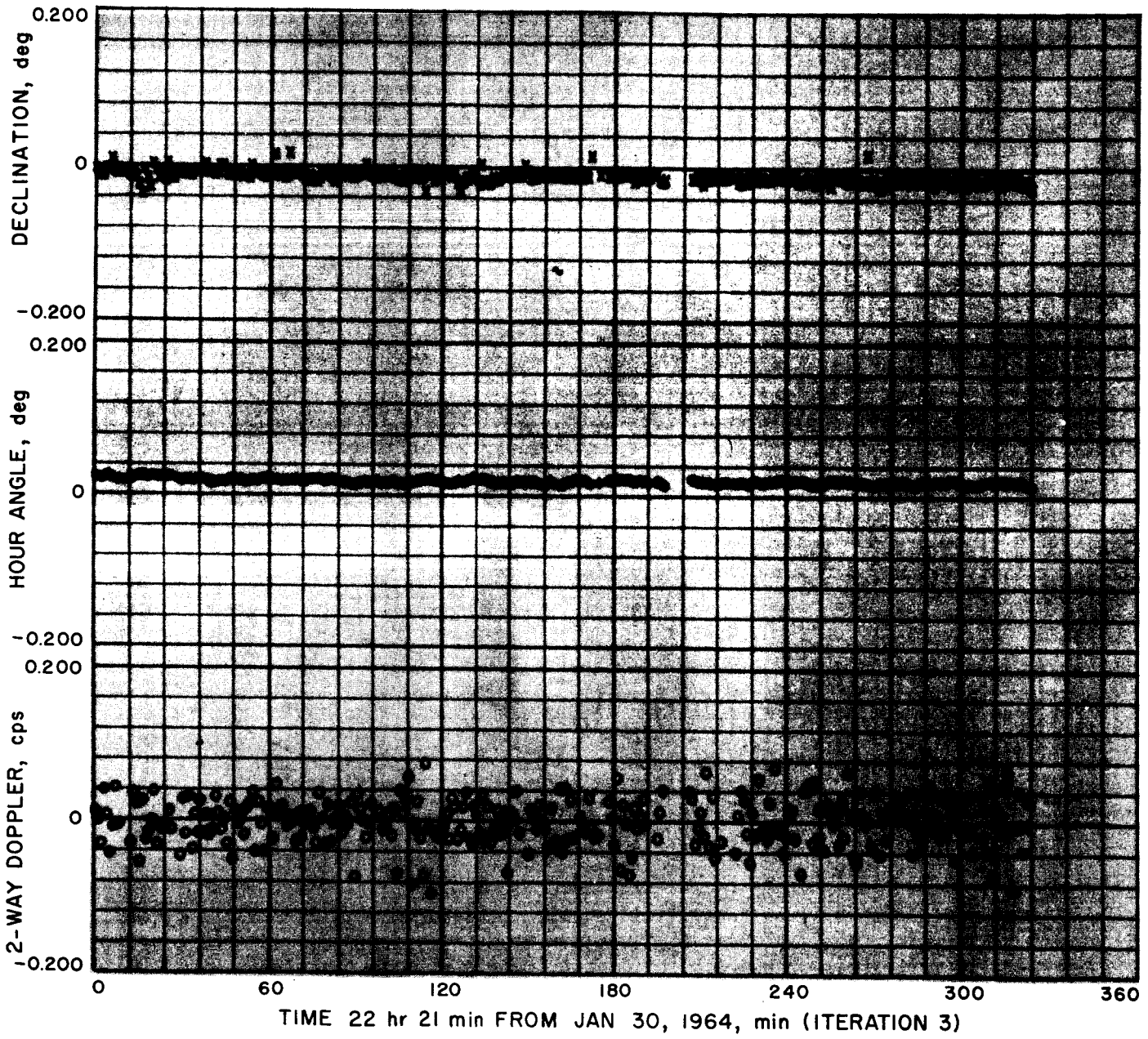

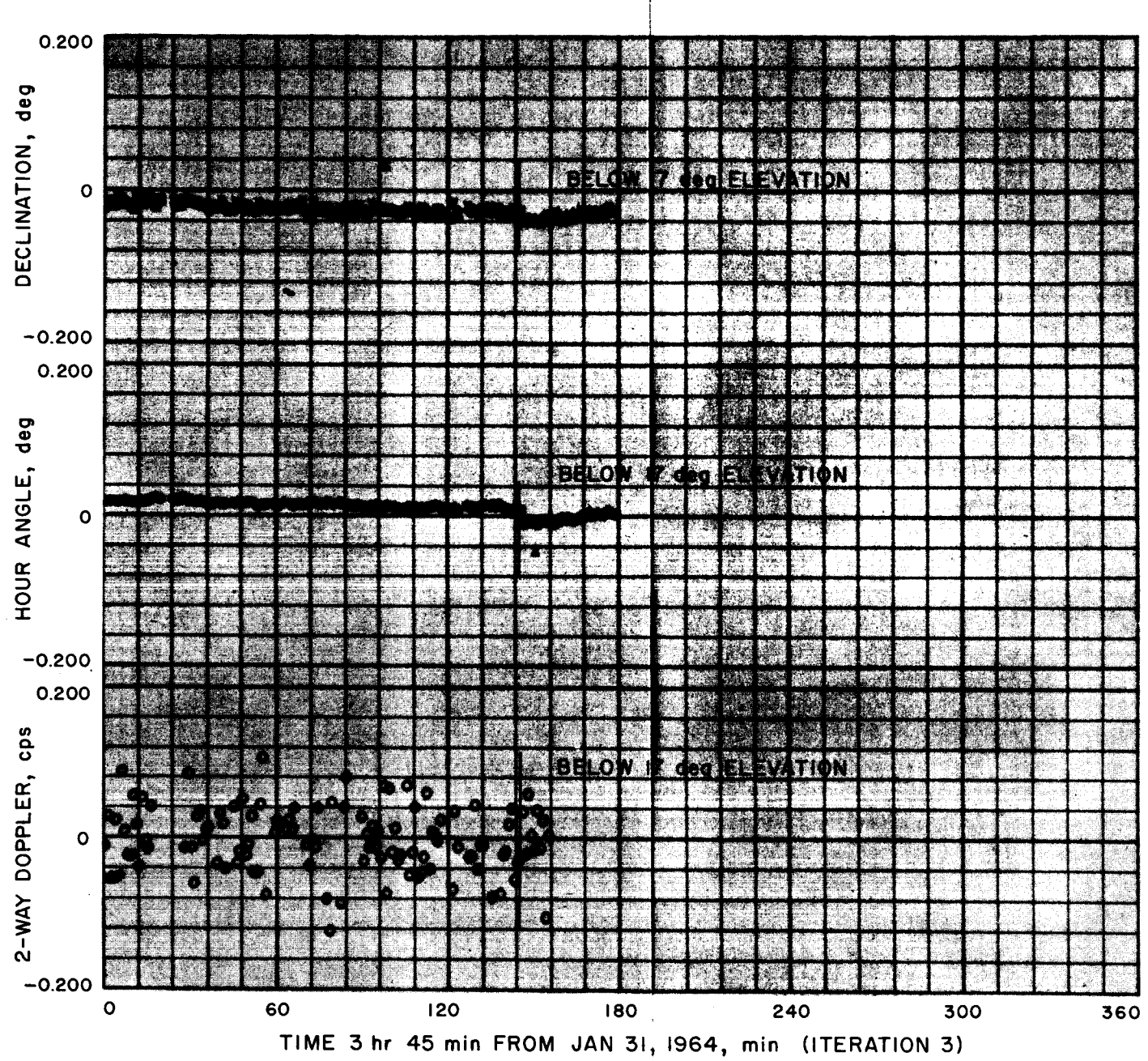

Figure 3. Station 51 Pass No. 01/303 Premaneuver Residuals*

*From Reference 2, pages 51-52

c) Transmitter drift caused by oscillator instability. Rubidium controlled oscillators at all stations have a nominal drift rate of 3 parts in 10^{11} per 1 hour.

Thus, the JPL statement of transmitter stability appears to be conservative, See for example McCourbrey, "Atomic Frequency Standards," Proceedings of the IEEE, February 1966, Volume 54, No. 2. Errors due to stability are entirely negligible over, say, 4-day periods. For longer periods; e.g., 40 days, the expected error due to drift is less than 0.03 cps. High frequency noise is illustrated in Figure 3 in which the deviations in the doppler residuals increase as the signal transit time increases (range increase). From this plot one may guess that this noise effect may be approximately the same order of magnitude, i.e., 10^{-2} cps rms.

d) Dropped or added cycles, caused by low signal-to-noise ratio and due to noise pulses being accepted as doppler cycle counts.

This noise source is mainly high frequency. Its magnitude may be estimated for an equivalent signal to noise ratio of 1 (very pessimistic) from

$$\delta f = \frac{3}{2\pi\tau} \frac{1}{(E/N)^{1/2}}$$

where τ is the count time duration, as

$$\delta f = \frac{3}{2\pi 60} < 10^{-2} \text{ cps}$$

---

* $$\delta f = \left(2\alpha^2 \frac{E}{N}\right)^{-1/2}$$

where α is the rms duration of the signal, and gives approximately the same answer as by considering a tight phase-lock-loop, which reads:

$$\delta f = \frac{\sqrt{2}}{\tau}\sqrt{\frac{1}{2E/N}}\left\{1 - e^{-\omega_n \tau\zeta}\left[\frac{\zeta(1 - 4\zeta^2)}{(1 + 4\zeta^2)\sqrt{1 - \zeta^2}} \sin\left(\alpha\sqrt{1 - \zeta^2}\right) + \cos\left(\alpha\sqrt{1 - \zeta^2}\right)\right]^{1/2}\right\}$$

where ω_n is the undamped loop natural frequency, ζ = damping factor.

(This last expression was derived from formulae given in "Fundamental Accuracy Limitations in a Two-Way Coherent Doppler Measurement System," by J. A. Develet, Jr., Trans. Ire, S.E. and T., September 1961.)

e) Variation in refraction correction which is due to differences between the atmospheric model used in the calculations and that which actually exists. This error source may be high or low frequency. The troposphere is modeled as simple spherical layers of varying density. As such, the effect becomes worse as the elevation decreases and increases with absolute elevation rate. Part of this effect at least, can be observed in the residual plots, Figures 4, 5, and 6 for elevation angles below 17 degrees. Thus while the model is certainly inadequate in that region, the magnitude of departure is rather small and occurs over a small region of data only.

The ionsphere may contribute an amount to the doppler effect, of a magnitude on the order of 10^{-2} cps which may show high and low frequency noise features with biases of the order 10^{-3} cps. (Figures are for average solar minimum conditions, cf, H. T. Howard et al., "Radar measurements of the cislunar medium," J. G. R. February 1, 1964 Volume 69, No. 3.) The ionosphere is not modeled in the JPL single precision program. The origin of the ionospheric contribution is the so-called dispersive doppler effect in which a varying electron density along the optical path of the radar signal causes a time varying phase advance and hence a frequency shift in the doppler data.

f) Antenna motion caused by spacecraft tumbling. The maximum contribution, assuming a satellite of scale length L and a spin frequency Ω is

$$\delta\dot{\rho} = \Omega L$$

The value of uncertainty would vary from mission to mission (dependent on success of maneuvering and propulsion phases). Considering present state-of-the-art, this quantity is almost certainly no higher than the other sources (10^{-2} cps). A typical value of Ω is 2×10^{-5} rad/sec and gives $\delta\dot{\rho} \sim 2 \times 10^{-3}$ cm/sec for $L = 10^2$ cm.

The RSS of the above error sources is less than $\sqrt{6} \times 10^{-2} \sim 0.025$ cps with perhaps a somewhat greater contribution from computer error which has been excluded from discussion here.

The second third, fourth and fifth error sources each contribute an approximate amount of 10^{-2} cps while other sources contribute lesser amounts with the exception of computation errors which do not show up in the residual plots.*

*The bias in the residual data was found to be negligible.

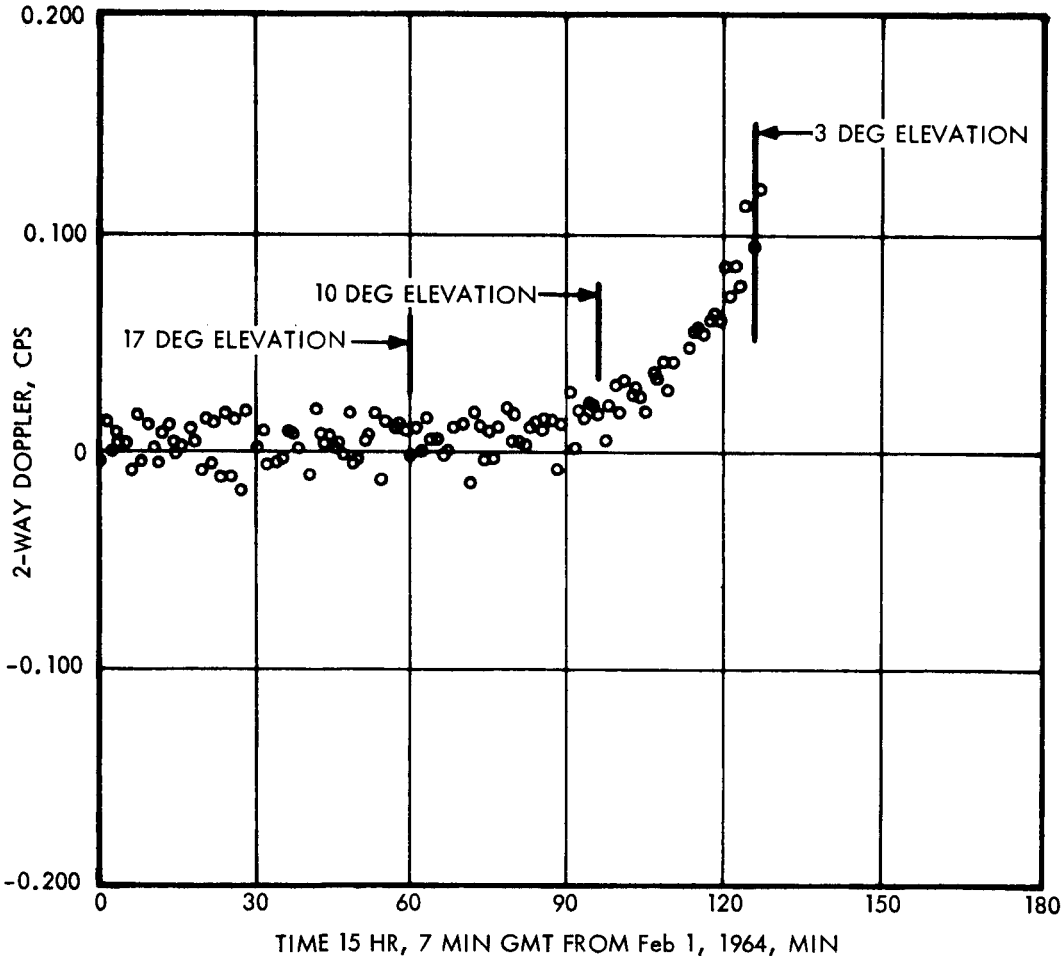

Figure 4. Residuals for Doppler Data Without ODP Refraction Model. (Elevation Rate ~ 0.245 deg/min)*

*See Reference 2

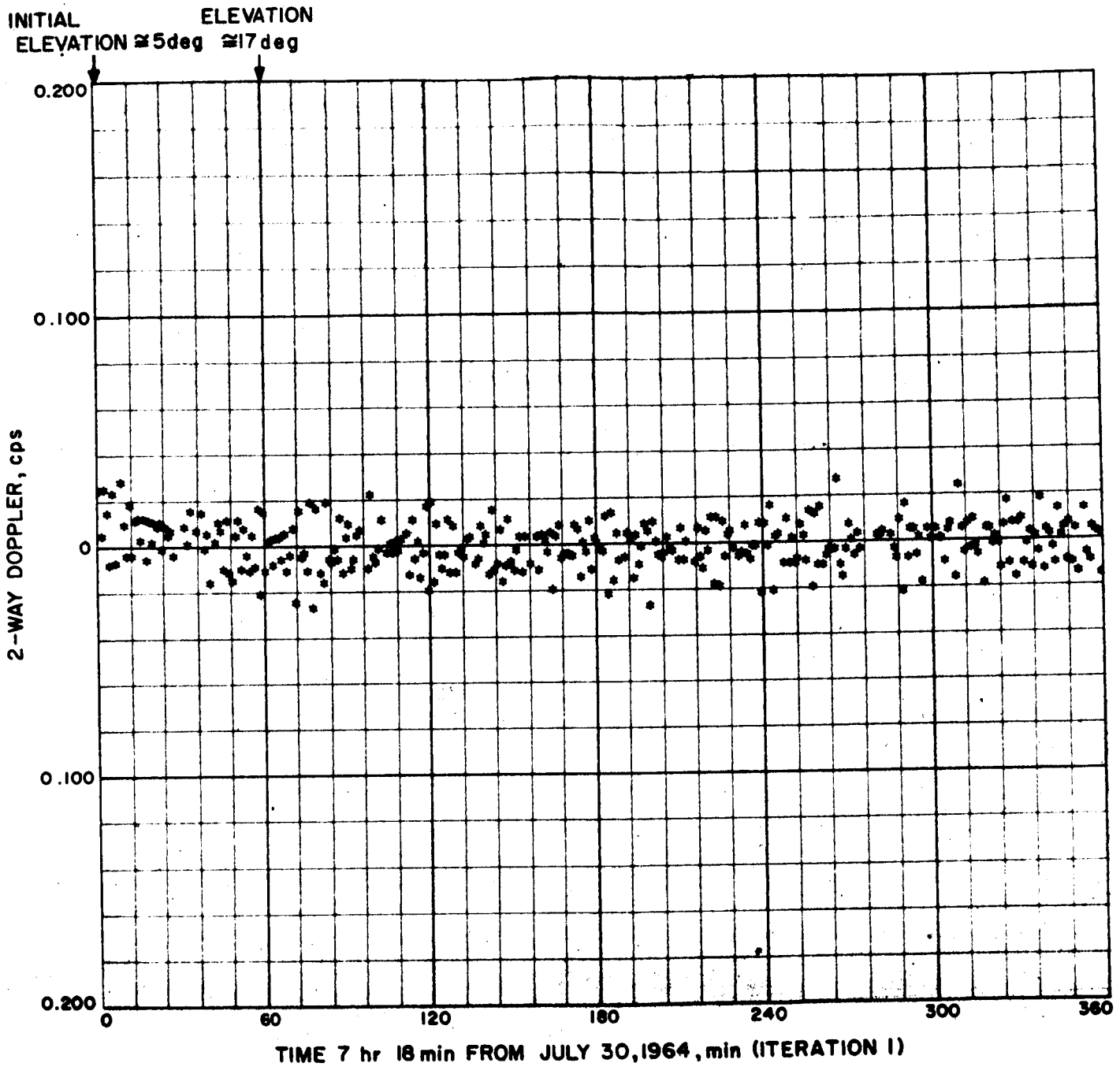

Figure 5. Station 12 Post Maneuver Pass No. 2 Two-Way Doppler Residuals (Start 07:18 GMT)*

*From Reference 1, page 29

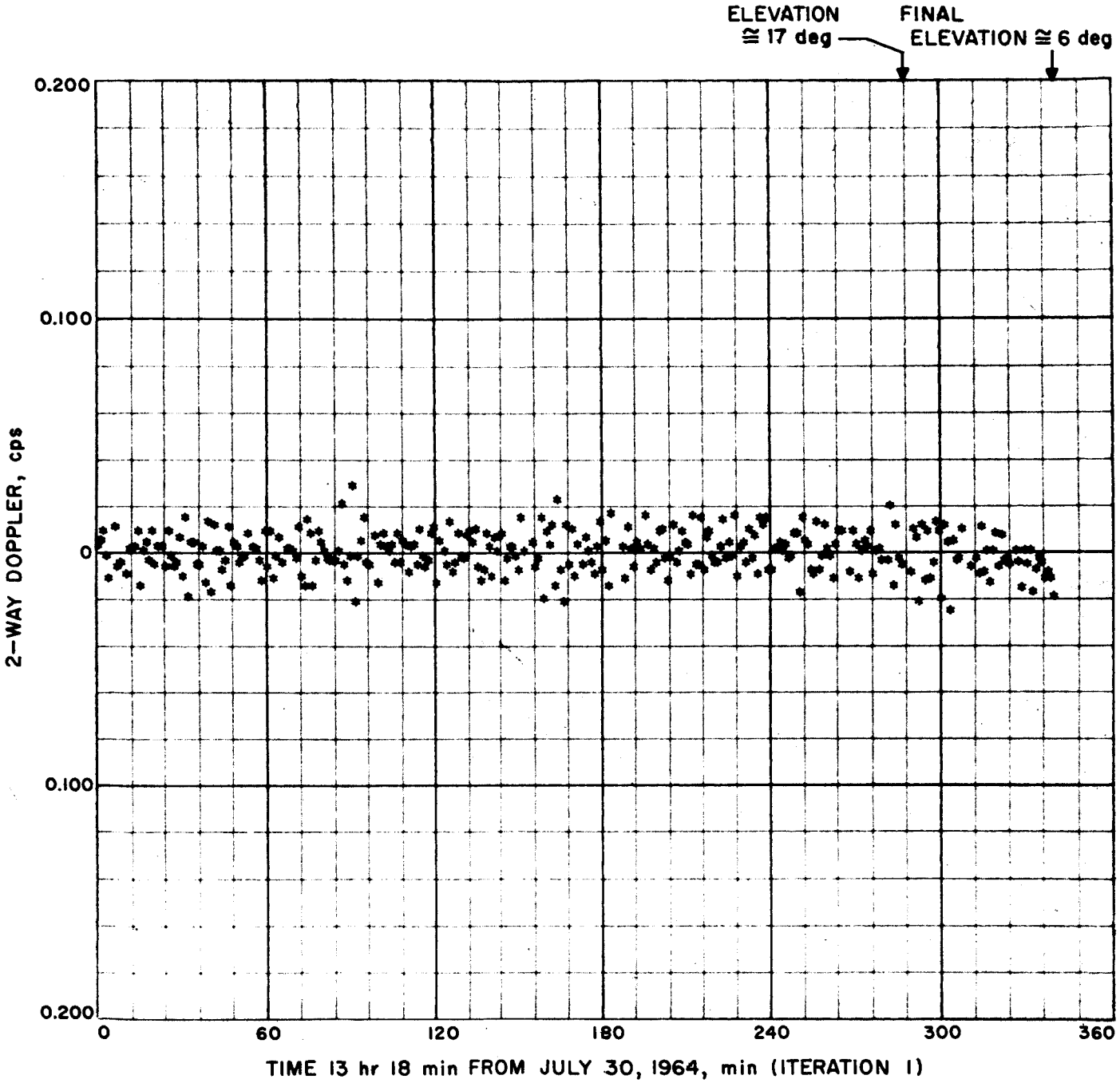

Figure 6. Station 12 Post Maneuver Pass No. 2 Two-Way Doppler Residuals (Start 13:18 GMT)*

*From Reference 1, page 30

(Analyses of these errors are considered elsewhere.) Thus, the theoretically expected errors are in agreement with experimentally derived errors (Tables II and III). Evidently, then, the a priori weights, while conservatives, are in accordance with theory and observation. (JPL's RSS weight was 0.088 cps.)

6. RELATIVISTIC EFFECTS ON TWO-WAY DOPPLER

The JPL single precision ODP neglects relativistic effects. To evaluate consequences of this omission we consider the relation between the received and transmitted frequency:*

$$\frac{\nu_o}{\nu_t} = \sqrt{\frac{1 + \frac{2\phi_t}{C^2} - \frac{V_t^2}{C^2}}{1 + \frac{2\phi_o}{C^2} - \frac{V_o^2}{C^2}}} \cdot \frac{1 - \frac{\dot{\vec{r}}_v \cdot (\vec{r}_v - \vec{r}_t)}{C\left|\vec{r}_v - \vec{r}_t\right|}\left(1 - \frac{2\phi_v}{C^2}\right)}{1 - \frac{\dot{\vec{r}}_t \cdot (\vec{r}_v - \vec{r}_t)}{C\left|\vec{r}_v - \vec{r}_t\right|}\left(1 - \frac{2\phi_t}{C^2}\right)} \cdot \frac{1 - \frac{\dot{\vec{r}}_o \cdot (\vec{r}_o - \vec{r}_v)}{C\left|\vec{r}_o - \vec{r}_v\right|}\left(1 - \frac{2\phi_o}{C^2}\right)}{1 - \frac{\dot{\vec{r}}_v \cdot (\vec{r}_o - \vec{r}_v)}{C\left|\vec{r}_o - \vec{r}_v\right|}\left(1 - \frac{2\phi_v}{C^2}\right)}$$

where

ν_o = the received RF frequency
ν_t = the transmitted RF frequency
ϕ_t = gravitational potential at transmitter
ϕ_o = gravitational potential at receiver
V_o = velocity of the receiver
V_t = velocity of the transmitter
$\vec{r}_v$ = vehicle position vector
$\vec{r}_o$ = receiver vehicle position vector
$\vec{r}_t$ = transmitter position vector

For two-way doppler the receiver and the transmitter are at the same physical location. Even considering a transit time of 2.5 seconds in which the station changes position, and its value of gravitational potential

*This expression for the doppler effect was computed for orbit determination by Dr. M. Payne in "General Relativistic Doppler Theory," MSC Internal Note No. 65-FM-90, June 1965.

changes very slightly, thus the quantities ϕ_t, ϕ_o, and V_t, V_o may be considered as equal to the accuracies of concern here. (These effects are the order of 10^{-5} cm/sec and less.) Thus, we have:

$$\frac{\nu_o}{\nu_t} = \frac{1 - \frac{|\dot{\vec{r}}_v|}{c} U_{vt}\left(1 - \frac{2\phi}{c^2}\right)}{1 - \frac{|\dot{\vec{r}}_t|}{c} U_{vt}\left(1 - \frac{2\phi}{c^2}\right)} \cdot \frac{1 - \frac{|\dot{\vec{r}}_o|}{c} U_{ov}\left(1 - \frac{2\phi}{c^2}\right)}{1 - \frac{|\dot{\vec{r}}_v|}{c} U_{ov}\left(1 - \frac{2\phi}{c^2}\right)}$$

Where U is the respective direction cosine. The potential term $\frac{2\phi}{c^2}$ is of the order of $(2 \times 10^3 / 9 \times 10^{10}) \approx 2 \times 10^{-8}$. Neglect of these terms has the approximate effect of multiplying the residuals by 2×10^{-8} (an error of two parts in $10^{-8} \sim 2 \times 10^{-2}$ mm/sec near the moon and 2×10^{-1} mm/sec near the earth, which would not be of interest in the present evaluation. Thus, for the two-way doppler situation considered here relativistic effects are negligible.

7. UNCERTAINTY CONTRIBUTED BY ASSIGNING A RANGE RATE INTERPRETATION TO THE COUNTED DOPPLER MEASUREMENT AND THE ASSIGNMENT OF TIME

In the JPL ODP, the doppler observable is represented as an instantaneous doppler frequency (tagged at the midpoint of the count interval) plus a correction term. Thus, the error caused by the assignment of a count rate interpretation (dividing the counts by the time interval), instead of doppler counts* as well as the proper assignment of time can be found by evaluating the first neglected term in the expansion. Consider the mathematical model used by JPL to represent the doppler observable* in explicit form.

The doppler observable, f, is given by

$$f = \frac{1}{\tau} \int_{t_{ob}-t/2}^{t_{ob}+\tau/2} F(t)\, dt$$

where

$$F(t) = \omega_3 + \omega_4 \nu_t \left(1 - \frac{\nu_o}{\nu_t}\right)$$

and

τ = the integration or count time

ω_3 = a bias frequency

ω_4 = multiplicative factor introduced at the S/C transponder to avoid jamming the receiver

ν_t = the transmitted frequency

ν_o = RF frequency at the receiver

*TRW Memo No. 3412.7-63

F(t) is now expanded in a Taylor series about the point t_{ob}. Thus, after integration, we are left with odd power terms only

$$f(t_{ob}) = \frac{1}{\tau}\left[F(t_{ob})\tau + \frac{F''(t_{ob})}{2!}\frac{\tau^3}{3} + \frac{F^{(iv)}(t_{ob})}{4!}\frac{\tau^5}{5} + \ldots\right]$$

$$= F(t_{ob}) + \frac{F''(t_{ob})}{2!}\frac{\tau^2}{3} + \frac{F^{(iv)}(t_{ob})}{4!}\frac{\tau^4}{5} + \ldots$$

where higher order terms have been omitted. The first and second terms are included in the ODP, with the exception of relativistic effects. We now evaluate the third term, retaining terms through $0(1/c)$ only.

Approximate values to use for the quantities of range and its derivatives up through order five were computed by considering the impact values of a free fall from infinity, which gives values approximately 40 percent higher than a circular orbit at the lunar surface. The direction of these quantities would be considered only if the value of a term computed without consideration of direction was significant.

The largest term computed on this basis was about 3×10^{-5} cm/sec (for t = 60 sec). This is about three orders of magnitude less than typical bias values found in Ranger VI and VII doppler residual data, and about two orders below the rms fluctuation in the same residual data. Thus, in comparison, the errors in time tagging and the method of representation of the observable contribute a negligible error.

8. CALCULATION OF QUANTIZATION OF COUNT AND COUNT RATE DATA

The quantization error in count data would be uniformly distributed between ±0.5 (apart from a constant). Thus

$$\sigma^2 = \int_{-1/2}^{1/2} x^2 \, dx = \frac{1}{12} \quad , \quad \sigma = \frac{1}{\sqrt{12}} \text{ cycles}$$

For the JPL S-Band system this is about 9 cm. For count-rate data

$$\sigma = \frac{1}{\tau} \frac{1}{\sqrt{12}}$$

where

$$\tau = 60 \text{ sec}$$
$$\sigma = 1.5 \times 10^{-2} \text{ cm/sec}$$

9. EFFECT OF BIAS ON DETERMINATION OF LUNAR GRAVITY

A lunar trajectory run was made on the TRW Systems ESPOD program and the inputed lunar constants were recovered with zero bias in range rate data. This corresponds to a possible bias and/or noise of 3×10^{-2} cm/sec or less, and the constants are recovered quite well. However, when the bias was increased to 10 cm/sec, the constants were not recovered with any accuracy at all. See Table II for details of the runs made with four and six iterations on a perfectly known a priori trajectory. It is concluded that reasonable accuracy should be obtained for the determined lunar constants.

TABLE II. —RUNS OF FOUR AND SIX ITERATIONS ON KNOWN "A PRIORI" TRAJECTORY*

	Trajectory Model	I = 4 Unbiased	I = 6 Bias = 10 cm/sec
x	2322.8116	2322.8120	2326.0022
y	99.162666	99.166294	104.44889
z	620.44467	620.44341	614.97155
$\dot{x}$	-0.58516493	-0.58516552	-0.58607167
$\dot{y}$	1.3472619	1.3472627	1.3465324
$\dot{z}$	0.37825414	0.37825074	0.37517479
C43	0.0	0.00002×10^{-4}	0.0057×10^{-4}
C44	0.017×10^{-4}	0.01699×10^{-4}	0.0008×10^{-4}
S21	0.0	0.0022×10^{-4}	1.146×10^{-4}
S31	0.21×10^{-4}	0.2102×10^{-4}	0.1030×10^{-4}
S41	0.54×10^{-4}	0.5378×10^{-4}	0.7734×10^{-4}
S22	0.0	0.0014×10^{-4}	0.1133×10^{-4}
S32	0.0	0.0001×10^{-4}	0.0794×10^{-4}
S42	0.0	0.0008×10^{-4}	0.0674×10^{-4}
S33	0.018×10^{-4}	0.01799×10^{-4}	0.0124×10^{-4}
S43	0.032×10^{-4}	0.03154×10^{-4}	0.0098×10^{-4}
S44	0.0	0.00004×10^{-4}	0.00095×10^{-4}

Initial estimate: $\Delta x, \Delta y, \Delta z = 0.5$ km
$\Delta \dot{x}, \Delta \dot{y}, \Delta \dot{z} = 0.5$ m/sec

Selenopotential: 0.0

*Runs made at TRW

10. RANGE MEASUREMENTS

The DSIF Ranging subsystem has the stated accuracy of a little better than ± 15 m. The system uses a coded plus and a correlation detector to measure the time of flight in terms of a cycle count of a stable reference oscillator. Since the inaccuracy is so large (due to delay in stabilization the transponder and ground equipment of about 0.03μs), the effect of the ionosphere is certainly negligible. After an initial range measurement, the doppler accumulator is used to provide the range information. Thus, it is seen that the range measurement functions more to provide a better initial estimate to the initial state vector at some epoch which is updated on succeeding iterations of the ODP. The important point, of course, is that the initial estimate be within the ODP convergence capabilities.

11. POWER SPECTRAL ANALYSIS

To explore the possibility that other effects of a nonrandom nature may be present in the residuals but unnoticed, a harmonic analysis of selected data was run. Although the noise was not found to be white, no significant peaking was noticeable (over the expected statistical fluctuation), and thus no strongly periodic phenomena seemed to be present.

A finer analysis would require much more data, a minimum of one thousand points perhaps, and more, if possible. Unless such quantities of data are available, reliable statistics are difficult to obtain. Due to time limitations and data condition, variations in the analysis to improve statistics was not employed. The autocovariance functions show that if the data is assumed to be exponentially correlated, then its time constant is less than one minute. Thus, there seems to be little value in pursuing this analysis further for the present case. Each of the following power spectrum autocorrelation plots are of doppler data taken from reference 2. In all cases, the equipment was operating on a rubidium standard, and the time series corresponding to Figure 7 is shown in Figure 5, and that corresponding to Figure 9 is shown in Figure 6.

10. RANGE MEASUREMENTS

The DSIF Ranging subsystem has the stated accuracy of a little better than 15 m. The system uses a coded pulse and a correlation detector to measure the time of flight in terms of a cycle count of a stable reference oxcillator. Since the inaccuracy is so large (due to delay in stabilization the transponder and ground equipment of about 0.03μs), the effect of the ionosphere is certainly negligible. After an initial range measurement, the doppler accumulator is used to provide the range information. Thus, it is seen that the range measurement functions more to provide a better initial estimate to the initial state vector at some epoch which is updated on succeeding iterations of the ODP. The important point, of course, is that the initial estimate be within the ODP convergence capabilities.

11. POWER SPECTRAL ANALYSIS

To explore the possibility that other effects of a nonrandom nature may be present in the residuals but unnoticed, a harmonic analysis of selected data was run. Although the noise was not found to be white, no significant peaking was noticeable (over the expected statistical fluctuation), and thus no strongly periodic phenomena seemed to be present.

A finer analysis would require much more data, a minimum of one thousand points perhaps, and more, if possible. Unless such quantities of data are available, reliable statistics are difficult to obtain. Due to time limitations and data condition, variations in the analysis to improve statistics was not employed. The autocovariance functions show that if the data is assumed to be exponentially correlated, then its time constant is less than one minute. Thus, there seems to be little value in pursuing this analysis further for the present case. Each of the following power spectrum autocorrelation plots are of doppler data taken from reference 2. In all cases, the equipment was operating on a rubidium standard, and the time series corresponding to Figure 7 is shown in Figure 5, and that corresponding to Figure 9 is shown in Figure 6.

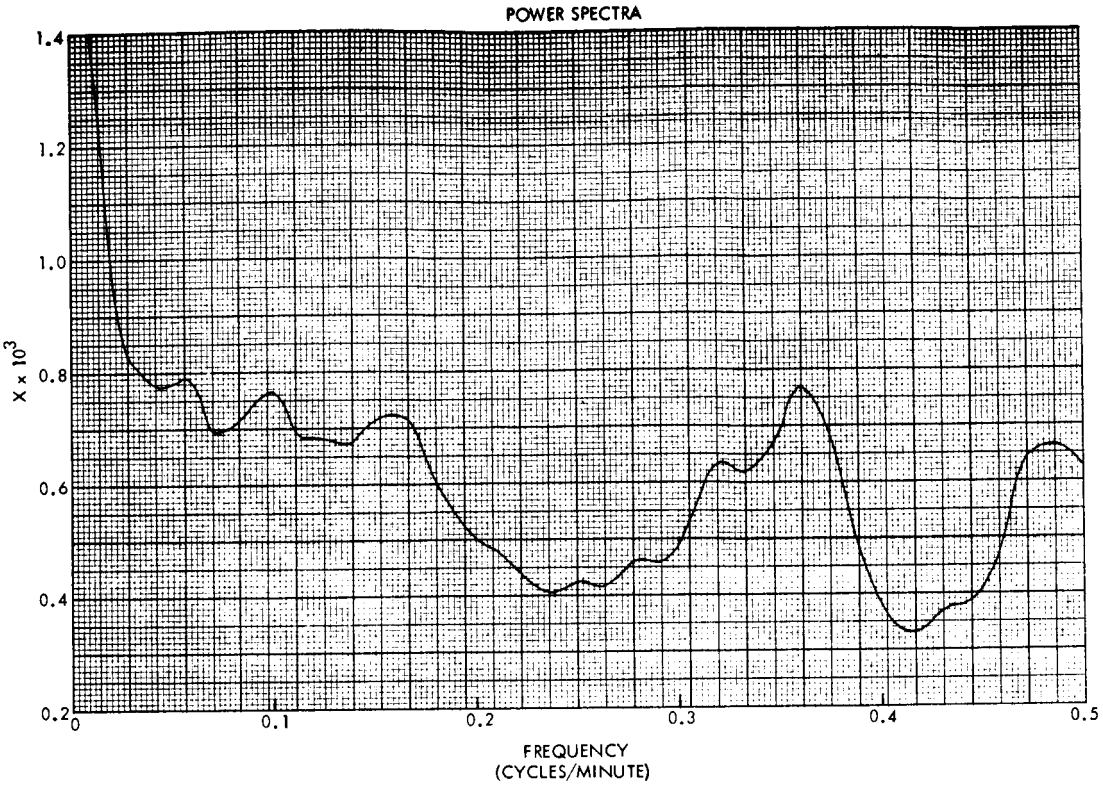

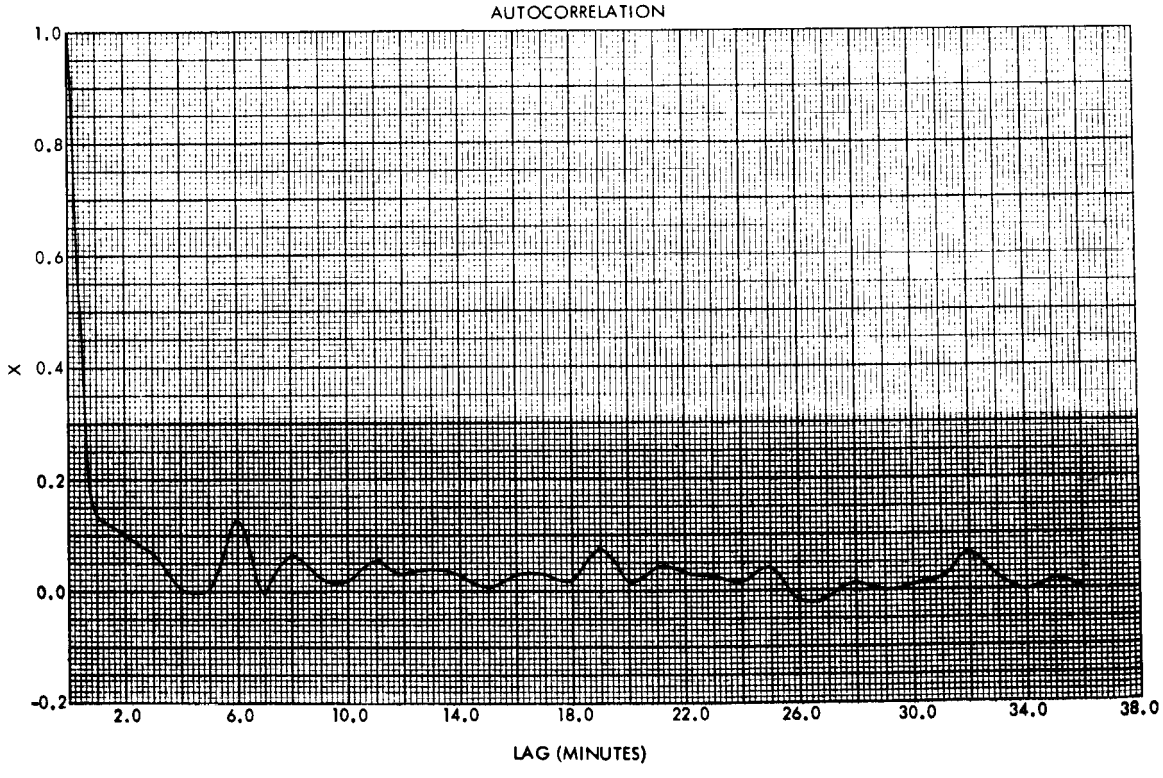

Figure 7. Power Spectra and Autocorrelation — Case 16

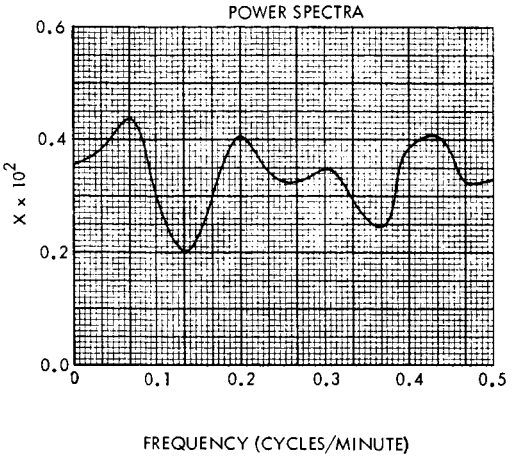

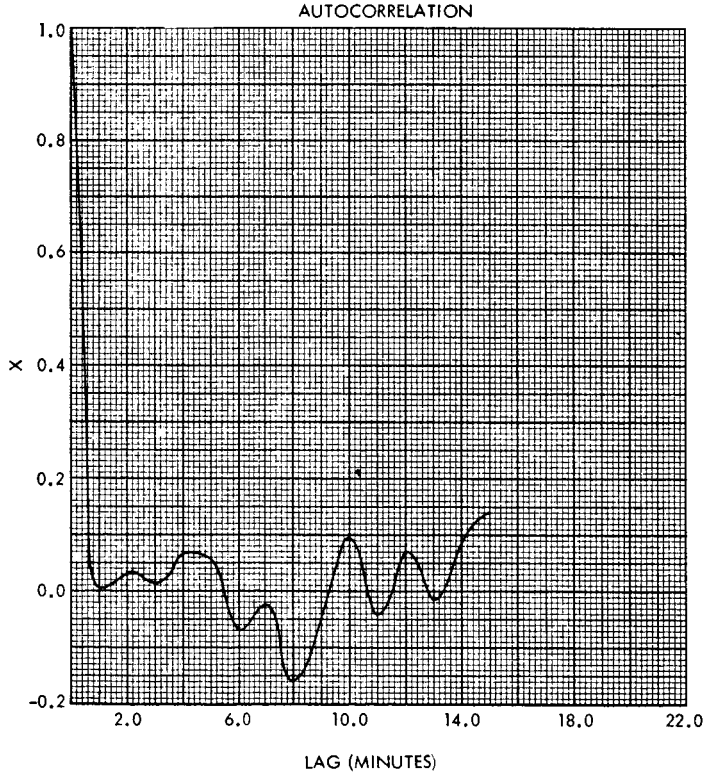

Figure 8. Power Spectra and Autocorrelation — Case 18

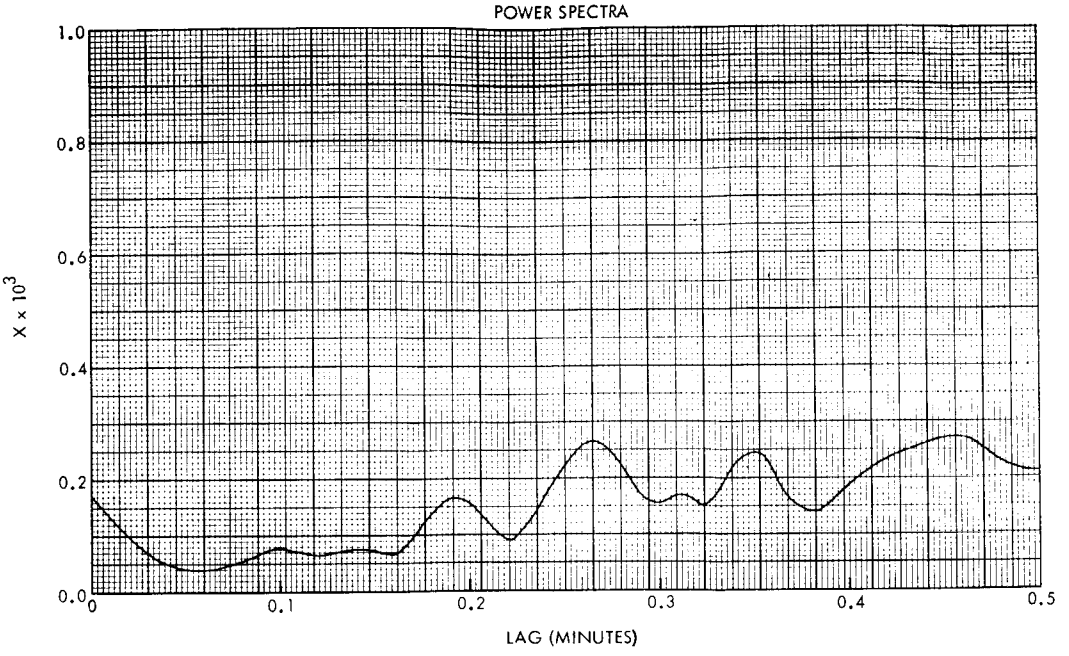

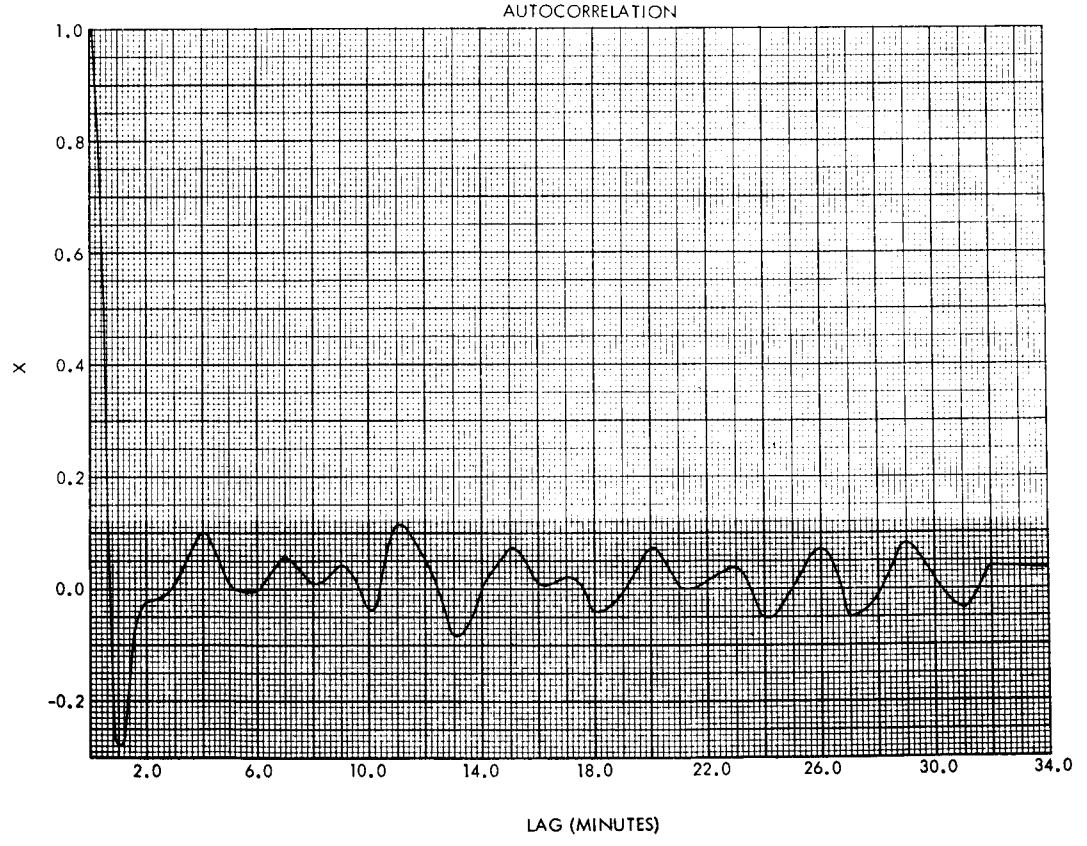

Figure 9. Power Spectra and Autocorrelation — Case 17

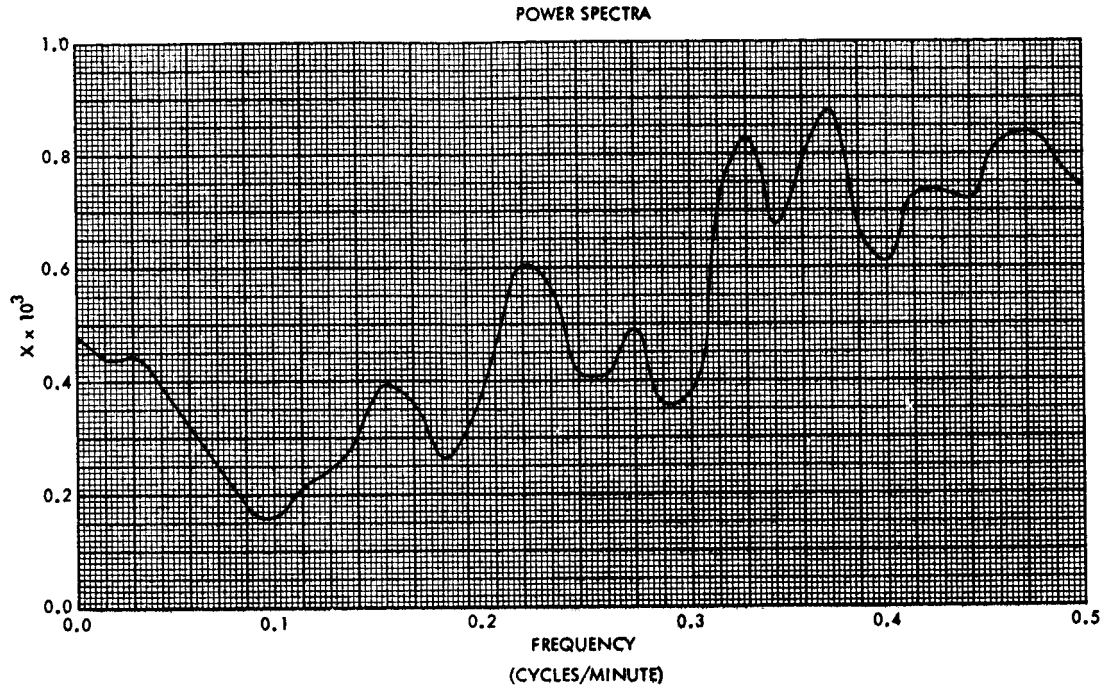

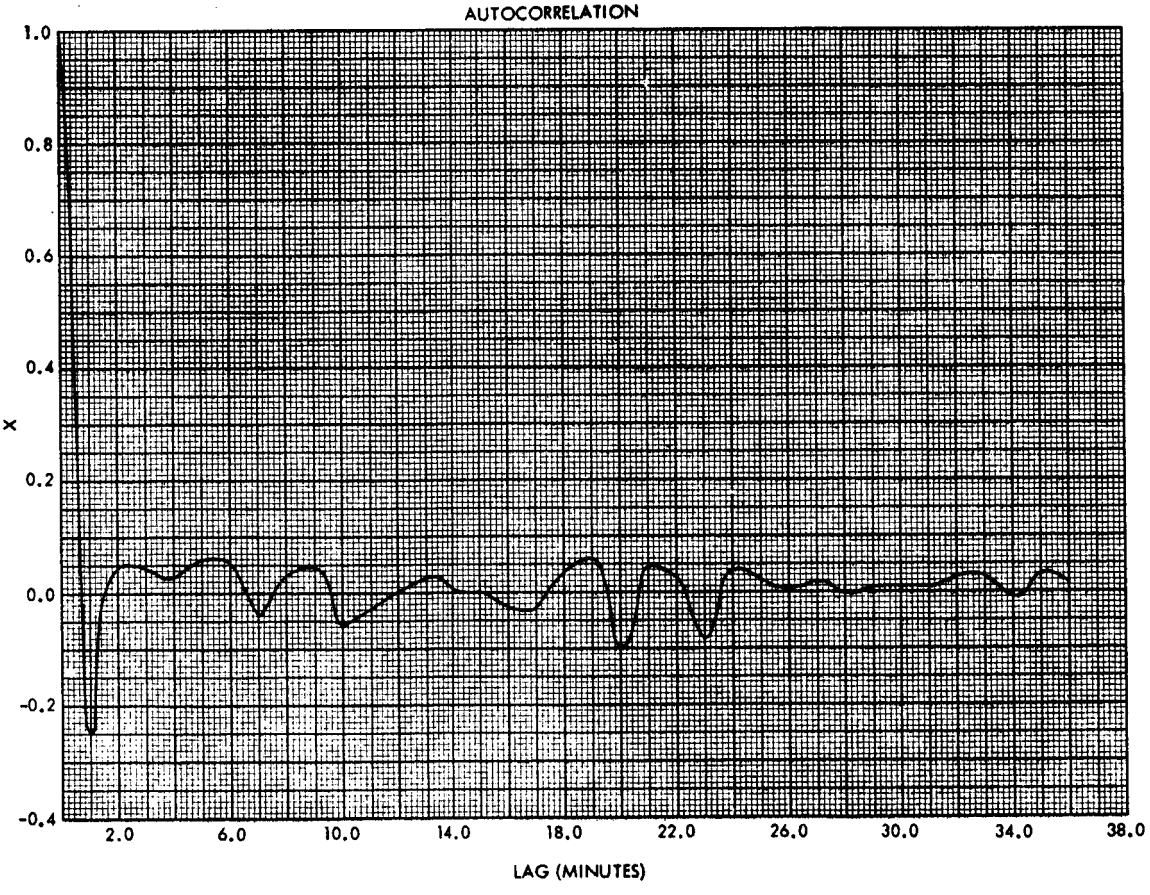

Figure 10. Power Spectra and Autocorrelation— Case 23

TABLE III. —STATISTICS ON POST MANEUVER DATA

Station	No a priority from premaneuver				With premaneuver data as a priority		With *REM* constraint	
	Number of doppler points	Standard deviation cps	Mean, cps	Remarks*	Standard deviation cps	Mean, cps	Standard deviation cps	Mean, cps
(1)	(2)	(3)	(4)	(5)	(6)	(7)	(8)	(9)
12	41	0.0220	0.0015	Pass No. 1, above 17 deg, not rubidium	0.0220	−0.0006	0.0222	−0.0004
	324	0.0093	0.0001	Pass No. 1, above 17 deg rubidium	0.0094	0.0012	0.0094	0.0013
	19	0.0130	−0.0029	Pass No. 1, below 17 deg, rubidium	0.0130	−0.0033	0.0133	−0.0036
	53	0.0120	0.0076	Pass No. 2, below 17 deg, rubidium	0.0120	0.0079	0.0120	0.0075
	543	0.0088	−0.0000	Pass No. 2, below 17 deg, rubidium	0.0088	−0.0005	0.0088	−0.0007
	71	0.0091	−0.0098	Pass No. 2, below 17 deg, rubidium	0.0090	−0.0089	0.0090	−0.0095
	54	0.0097	0.0018	Pass No. 3, below 17 deg, rubidium	0.0099	0.0063	0.0098	0.0051
	57	0.0087	−0.0009	Pass No. 3, above 17 deg, rubidium	0.0089	0.0008	0.0091	−0.0013
	11	0.0140	−0.0077	Pass No. 3, above 17 deg, not rubidium	0.0130	−0.0098	0.0133	−0.0138
	20	0.0087	−0.0001	Pass No. 3, above 17 deg, rubidium	0.0088	−0.0047	0.0089	−0.0122
	35	0.0250	−0.0012	Pass No. 3, above 17 deg, not rubidium	0.0350	0.0134	0.0332	−0.0268
	12	0.2110	−0.0487	Pass No. 3, above 17 deg, not rubidium (5-sec count)	0.2070	−0.0779	0.2060	−0.2340
41	259	0.0330	−0.0011	Pass No. 1, above 17 deg, not rubidium	0.0280	−0.0018	0.0333	−0.0001
	146	0.0510	0.0042	Pass No. 2, above 17 deg, not rubidium	0.0470	−0.0004	0.0515	0.0060
51	397	0.0277	+0.0006	Pass No. 1, above 17 deg, not rubidium	0.0276	−0.0018	0.0276	−0.0022
	264	0.0471	−0.0005	Pass No. 2, above 17 deg, not rubidium	0.0473	−0.0045	0.0473	−0.0009

0.01 cps = 0.00156 m/sec

*17 deg was chosen as a point above which uncertainties in atmospheric effects would be negligible. Rubidium standards are available at Station 12; Stations 41 and 51 do not have the equipment. The remarks are made primarily for data weighting considerations (Appendix B).

TABLE IV. —VALUES OF ESTIMATED PARAMETERS AT MANEUVER EPOCH*

Parameters estimated (1)	Units (2)	Nominals (3)	Premaneuver, no a priority from postmaneuver (4)	Postmaneuver, no a priority from premaneuver (5)	Postmaneuver with a priority from premaneuver (6)	Premaneuver with a priority from postmaneuver (7)	With *REM* constraint (8)
X	km	—	−169638.82	−169642.14	−169640.40	−169639.09	−169640.40
Y	km	—	−2928.1380	−2928.9956	−2928.6339	−2928.4060	−2928.4773
Z	km	—	−10683.048	−10671.608	−10676.441	−10676.529	−10676.566
DX	m/sec	—	−1845.1682**	−1807.8626**	−1807.8720**	−1845.1674**	−1807.8724**
DY	m/sec	—	−404.16339	−395.24578	−395.22410	−404.16908	−395.22270
DZ	m/sec	—	85.245439	100.46492	100.45332	85.313467	100.45143
$GM_{\oplus}$	km^3/sec^2	398603.20	398603.04	398603.75	398600.63	398600.75	398600.61
$GM_{\leftmoon}$	km^3/sec^2	4902.7779	4902.7441	4902.6332	4902.6293	4902.6664	4902.6182
REM	km	6378.3254	6378.3254	6378.3147	6378.3095	6378.3039	6378.3111
GB	—	0.4	0.3986	0.4045	0.3868	0.391	0.3889
Station 12							
Radius	km	6372.0164	6371.8849	6371.8792	6371.8770	6371.8776	6371.8773
Latitude	deg	35.116540	35.117368	35.117409	35.117400	35.117402	35.117400
Longitude	deg	243.19539	243.19508	243.19463	243.19428	243.19435	243.19422
Station 41							
Radius	km	6372.6076	6372.7126	6372.6432	6372.6040	6372.6112	6372.6042
Latitude	deg	−31.212360	−31.211811	−31.212164	−31.211875	−31.211914	−31.211876
Longitude	deg	136.88617	136.88659	136.88775	136.88727	136.88729	136.88722
Station 51							
Radius	km	6375.5503	6375.5232	6375.4930	6375.4980	6375.4991	6375.4976
Latitude	deg	−25.738763	−25.738862	−25.739014	−25.739277	−25.739260	−25.739268
Longitude	deg	27.685588	27.685466	27.685576	27.685181	27.685219	27.685129

*Maneuver epoch was 08:57:09.000 GMT January 31, 1964.

**The differences in velocity components are due to the maneuver; premaneuver conditions are before the maneuver while postmaneuver are after the maneuver. This is also true of position, but the changes are not as dramatic, since positional changes are on the order of < 1 km.

*From Reference 2, page 14

12. SPACE PLASMA EFFECTS

The only possibly significant effect in this area is again the dispersive doppler effect. However, its magnitude outside the earth's magnetosphere is many orders of magnitude below that found for the ionosphere which is, itself, negligible. Even if the moon possessed a magnetosphere or created a wake in the streaming plasma (the solar winds), it is highly unlikely that its magnitude could compare in any way to that of the earth's ionosphere (Russian magnetic measurements).

13. CONCLUSIONS

The conclusions reached, then, in this brief analysis are that the DSIF has apparently exceeded its stated capabilities, and has the capability to perform adequately in the Lunar Orbiter studies, including the solution for lunar potential contants.

14. BIBLIOGRAPHY

1. W. R. Wollenhaupt, et al., "Ranger VII Flight Path and Its Determination From Tracking Data," JPL Technical Report No. 32-694.

2. W. L. Sjogren, et al., "The Ranger VI Flight Path and Its Determination From Tracking Data," JPL Technical Report No. 32-605.

NASA CR-66246

DISTRIBUTION LIST

NAS1-4605-7

		Copies
NASA Langley Research Center Langley Station Hampton, Virginia 23365		
Attention:	Contracting Officer	1
	W. H. Phillips, Mail Stop 310	1
	R. H. Tolson, Mail Stop 304	1
	A. P. Mayo, Mail Stop 248	1
	Normal L. Crabill, Mail Stop 159	1
	W. T. Blackshear, Mail Stop 304	1
	James J. Buglia, Mail Stop 214A	1
	Library, Mail Stop 185	1
	R. L. Zavasky, Mail Stop 117	1
NASA Ames Research Center Moffett Field, California 94035		
Attention:	Library	1
	John S. White	1
NASA Flight Research Center P. O. Box 273 Edwards, California 93523		
Attention:	Library	1
NASA Goddard Space Flight Center Greenbelt, Maryland 20771		
Attention:	Library	1
	Arthur J. Fuchs, Code 554	1
Jet Propulsion Laboratory 4800 Oak Grove Drive Pasadena, California 91103		
Attention:	Library	1
	Joseph Brenkle	1
NASA Manned Spacecraft Center Houston, Texas 77001		
Attention:	Library	1
	Emil R. Schiesser, Code FM4	1
NASA Marshall Space Flight Center Huntsville, Alabama 35812		
Attention:	Library	1
	Dr. Walter Haeussermann	1
NASA Western Operations 150 Pico Boulevard Santa Monica, California 90406		
Attention:	Library	1

NASA CR-66246

DISTRIBUTION LIST

NAS1-4605-7

	Copies
NASA Wallops Station Wallops Island, Virginia 23337 Attention: Library	1
NASA Electronics Research Center 575 Technology Square Cambridge, Massachusetts 02139 Attention: Library Richard J. Hayes, Chief, Guidance Laboratory	1 1
NASA Lewis Research Center Mail Stop 3-7 2100 Brookpark Road Cleveland, Ohio 44135	1
NASA John F. Kennedy Space Center Kennedy Space Center, Florida 32899 Attention: Code ATS-132	1
NASA Michoud Assembly Facility P. O. Box 26078 New Orleans, Louisiana 70126 Attention: Mr. Henry Quintin, Code I-Mich-D	1
National Aeronautics and Space Administration Washington, D. C. 20546 Attention: Library, Code USS-10 Capt. Lee R. Scherer, Code SL	1 1
NASA Scientific and Technical Information Facility P. O. Box 33 College Park, Maryland 20740	16 plus reproducible